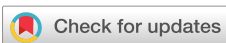


RESEARCH ARTICLE | FEBRUARY 28 2023

## High conductivity and low activation energy in p-type AlGaN



Shashwat Rathkanthiwar ; Pegah Bagheri; Dolar Khachariya; ... et. al



*Appl. Phys. Lett.* 122, 092103 (2023)

<https://doi.org/10.1063/5.0141863>



View  
Online



Export  
Citation

CrossMark



Time to get excited.  
Lock-in Amplifiers – from DC to 8.5 GHz



Find out more



Zurich  
Instruments

# High conductivity and low activation energy in p-type AlGaN

Cite as: Appl. Phys. Lett. **122**, 092103 (2023); doi: [10.1063/5.0141863](https://doi.org/10.1063/5.0141863)

Submitted: 9 January 2023 · Accepted: 15 February 2023 ·

Published Online: 28 February 2023



View Online



Export Citation



CrossMark

Shashwat Rathkanthiwar,<sup>1,a)</sup> Pegah Bagheri,<sup>1</sup> Dolar Khachariya,<sup>2</sup> Seiji Mita,<sup>2</sup> Cristyan Quiñones-García,<sup>1</sup> Yan Guan,<sup>1</sup> Baxter Moody,<sup>2</sup> Pramod Reddy,<sup>2</sup> Ronny Kirste,<sup>2</sup> Ramón Collazo,<sup>1</sup> and Zlatko Sitar<sup>1,2</sup>

## AFFILIATIONS

<sup>1</sup>Department of Materials Science and Engineering, North Carolina State University, Raleigh, North Carolina 27695-7919, USA

<sup>2</sup>Adroit Materials, Inc., 2054 Kildaire Farm Rd., Cary, North Carolina 27518, USA

<sup>a)</sup>Author to whom correspondence should be addressed: [srathka@ncsu.edu](mailto:srathka@ncsu.edu)

## ABSTRACT

Record-low p-type resistivities of 9.7 and 37  $\Omega$  cm were achieved in  $\text{Al}_{0.7}\text{Ga}_{0.3}\text{N}$  and  $\text{Al}_{0.8}\text{Ga}_{0.2}\text{N}$  films, respectively, grown on single-crystal AlN substrate by metalorganic chemical vapor deposition. A two-band conduction model was introduced to explain the anomalous thermal behavior of resistivity and the Hall coefficient. Relatively heavy Mg doping ( $5 \times 10^{19} \text{ cm}^{-3}$ ), in conjunction with compensation control, enabled the formation of an impurity band exhibiting a shallow activation energy of  $\sim 30 \text{ meV}$  for a wide temperature range. Valence band conduction associated with a large Mg ionization energy was dominant above 500 K. The apparently anomalous results deviating from the classical semiconductor physics were attributed to fundamentally different Hall scattering factors for impurity and valence band conduction. This work demonstrates the utility of impurity band conduction to achieve technologically relevant p-type conductivity in Al-rich AlGaN.

Published under an exclusive license by AIP Publishing. <https://doi.org/10.1063/5.0141863>

Al-rich aluminum gallium nitride (AlGaN) alloys are promising compound semiconductors for deep-ultraviolet (DUV) optoelectronics, thanks to their direct and tunable ultrawide bandgap. Owing to their small size, low weight, low operating power, and robustness, AlGaN-based DUV light-emitting diodes and laser diodes are poised to replace traditional Hg-based UV sources for point-of-use water purification, biological/chemical sensing, air-disinfection, surface sterilization, medical treatments, and materials processing.<sup>1</sup> They are also expected to enable a host of other optoelectronic applications, such as quantum computing, lithography sources, non-line-of-sight communication, micromachining, atomic clocks, etc.<sup>2</sup> The performance of these optical devices has been limited by the challenges associated with achieving low resistivity p-type AlGaN layers.

Although Mg remains the most promising p-type dopant in AlGaN, the relatively high ionization energy increasing from  $\sim 150 \text{ meV}$  ( $\text{GaN}$ )<sup>3</sup> to  $\sim 600 \text{ meV}$  ( $\text{AlN}$ )<sup>12</sup> imposes a fundamental bottleneck for achieving a high free hole concentration. Figure 1 shows the reported resistivity values for p-AlGaN films grown by metalorganic chemical vapor deposition (MOCVD).<sup>3–11</sup> Expectedly, the resistivity increases exponentially with Al content. We note that these values correspond to AlGaN films grown with constant composition and doping concentration. While alternate doping approaches such as short period superlattices,<sup>13,14</sup> composition modulation,<sup>15</sup> and Mg delta doping<sup>16</sup> allow for low

lateral resistivity in p-AlGaN, the vertical conduction is limited due to the barriers associated with the periodic oscillation of the energy bands.<sup>17</sup> The polarization-graded AlGaN approach, on the other hand, necessitates the grading toward Ga-rich compositions to achieve high hole concentration and to favor the Ohmic contact formation.<sup>18–20</sup> This approach suffers from UV-C absorption loss in the p-type layer, significantly decreasing the light extraction efficiency in optoelectronic devices. Therefore, it is of significance to devise techniques for achieving low p-type resistivity in Al-rich AlGaN without modulating the composition or the doping profile.

In addition to the high acceptor ionization energy, the enhanced incorporation of compensating point defects with increasing bandgap<sup>21,22</sup> makes p-doping of Al-rich AlGaN a formidable challenge. Recently, Bagheri *et al.*<sup>9</sup> reported a significant improvement in resistivity for 60% AlGaN films ( $10 \Omega \text{ cm}$ ) by reducing the compensation and employing a relatively heavy Mg doping ( $5 \times 10^{19} \text{ cm}^{-3}$ ). While the dislocation-related compensation was avoided by using single-crystal AlN substrates, the nitrogen-vacancy-related compensation was controlled by using high nitrogen chemical potential growth conditions.<sup>23,24</sup> Previously, Nakarmi *et al.*<sup>25</sup> had also observed the suppression in impurity transitions associated with nitrogen-vacancy in  $\text{Mg:Al}_{0.7}\text{Ga}_{0.3}\text{N}$  by increasing the V/III ratio during the growth. Similarly, Kinoshita *et al.*<sup>11</sup> reported on the reduction in the intensity

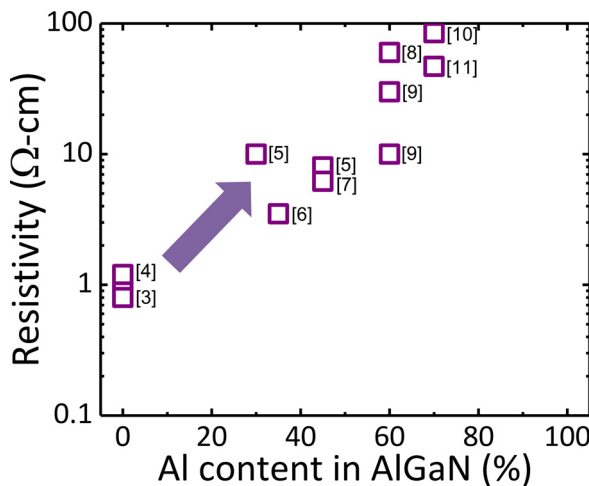


FIG. 1. Literature overview of resistivity values reported for p-AlGaN films grown by MOCVD with constant composition and doping concentration.<sup>3–11</sup>

of nitrogen-vacancy-related 4.1 eV photoluminescence peak in Mg:Al<sub>0.7</sub>Ga<sub>0.3</sub>N when the V/III ratio was increased, which helped them to achieve a resistivity of 47 Ω cm. Interestingly, Bagheri *et al.*<sup>9</sup> and Kinoshita *et al.*<sup>11</sup> reported on temperature-dependent resistivity with ionization energies below 50 meV, which is much lower than the expected Mg ionization energy for Al-rich AlGaN. The observed low resistivity was attributed to the impurity band conduction in the relatively heavily doped AlGaN films.

In this Letter, we develop a model for understanding impurity band conduction in Mg-doped AlGaN and demonstrate the utility of this conduction mechanism to achieve reproducibly technologically relevant resistivities in Al-rich p-AlGaN films.

A relatively heavy Mg doping of  $5 \times 10^{19} \text{ cm}^{-3}$  was investigated in this study for AlGaN films grown with three different Al contents: 0% (GaN), 70% (Al<sub>0.7</sub>Ga<sub>0.3</sub>N), and 80% (Al<sub>0.8</sub>Ga<sub>0.2</sub>N). The samples were grown on 1-in. (0001) single-crystal AlN substrates using a vertical, cold-walled, low-pressure, RF-heated MOCVD reactor at a total pressure of 20 Torr. The 500 μm thick substrates were processed from AlN single-crystalline boules grown by physical vapor transport.<sup>26,27</sup> The wafers had an average threading dislocation density (TDD)  $<10^3 \text{ cm}^{-2}$ , and a miscut of 0.2° toward the m-direction. Pre-epitaxy acid-based AlN surface preparation, hydrogen annealing, and nitridation are described elsewhere.<sup>28</sup> Trimethylaluminum (TMA), triethylgallium (TEG), ammonia (NH<sub>3</sub>), and bis-cyclopentadienyl magnesium (Cp<sub>2</sub>Mg) were used as the precursors for Al, Ga, N, and Mg, respectively. The growth temperature and V/III ratio employed for the growth of Mg-doped GaN (Al-rich AlGaN) were 1315 K (1375 K) and 2000 (2900), respectively, while the thickness was 200 nm. A sample consisting of 200 nm-thick p-GaN with a lower Mg doping concentration of  $2 \times 10^{19} \text{ cm}^{-3}$  was grown on sapphire substrate under similar growth conditions and was used as a reference sample for the Hall studies.

The Al-content in the AlGaN films was determined using x-ray diffraction (XRD) measurements using a Philips X'Pert materials research diffractometer.<sup>29</sup> The Mg activation-anneal was performed in a rapid thermal annealing system at 975 K, under air ambient for

10 min. Ni/Au (20/40 nm) contacts were deposited using e-beam evaporation and patterned in the van der Pauw geometry for electrical measurements. The contacts were annealed at 875 K for 10 minutes under air ambient for Ohmic contact formation. Temperature-dependent resistivity and Hall measurements were performed in a temperature range of 200–700 K using a Lake Shore 8400 series AC/DC Hall measurement system at high applied biases  $>50$  V. An alternating magnetic field was coupled with a lock-in amplifier for an accurate determination of the Hall coefficients in low-mobility samples.

Based on the previously reported observations described in the introduction, a model for impurity band conduction in Mg-doped AlGaN is developed and validated based on the experiments described in this Letter. Due to the large ionization energy, it is expected that only a minor fraction of the Mg dopants ionizes at room temperature (RT), whereas the majority of Mg dopants remain in a neutral configuration. At relatively low doping concentrations ( $<5 \times 10^{18} \text{ cm}^{-3}$ ), the Mg dopants can be considered to be isolated and non-interacting (Fig. 2, left). The only route for conduction is via ionization of Mg impurities, followed by the hole transport in the valence band. As the Mg concentration increases but is still well below the Mott transition, the Mg dopants begin to interact, and the carrier transport may occur via a multi-phonon hopping process involving tunneling,<sup>30</sup> which is associated with the overlap of the atomic wavefunctions of initial and final atomic configurations<sup>31</sup> (Fig. 2, center). At even higher Mg doping concentrations ( $>5 \times 10^{19} \text{ cm}^{-3}$ ), but still below the Mott transition, the overlap of the dopant states can cause the dopant energy level to split into a quasi-continuous impurity band (Fig. 2, right). This

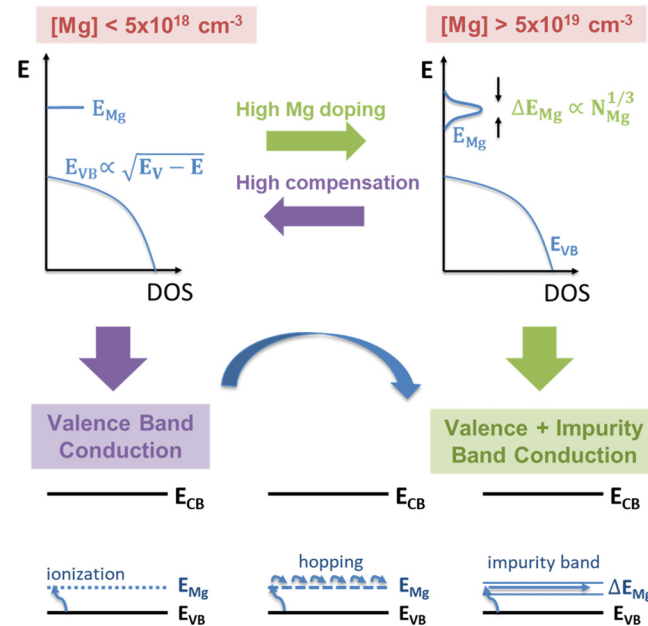
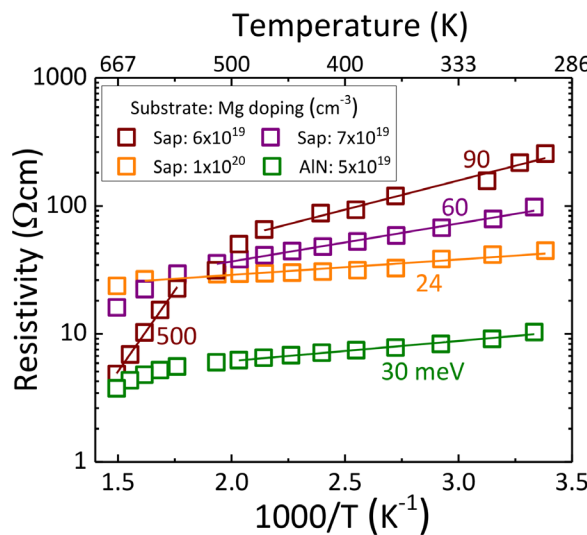


FIG. 2. (Top) A schematic of the density of states showing the evolution of the Mg acceptor level to a band at low compensation and high doping concentrations. (Bottom) Simplistic band diagram illustrating the viable conduction routes for low (Mg ionization followed by valence band conduction), moderate (valence band conduction and hopping conduction along Mg states), and high (valence band conduction and Mg impurity band conduction) doping levels at low compensation.



**FIG. 3.** Temperature-dependent resistivity for p-Al<sub>0.6</sub>Ga<sub>0.4</sub>N doped with varied Mg doping concentrations and grown on sapphire and AlN substrates. Reproduced with permission from Bagheri *et al.*, *Appl. Phys. Lett.* **120**, 082102 (2022). Copyright 2022 AIP Publishing.

provides an alternate route for conduction, where the carriers can propagate through the impurity band with a much-reduced activation energy as compared to the relatively large Mg ionization energy required for the valence band transport. As pointed out by Neumann,<sup>32</sup> the effect of impurity band conduction becomes more pronounced with increasing acceptor ionization energy. This explains the impurity band conduction observed in Mg-doped GaN<sup>33</sup> and Al-rich AlGaN<sup>9–11</sup> films at relatively high doping concentrations,  $>4 \times 10^{19} \text{ cm}^{-3}$ .

It is worthwhile to note that the presence of compensating point defects can disrupt the overlap of the Mg orbitals and, hence, impede the formation of the impurity band. The relatively high Mg ionization energy in AlGaN typically imposes a high Mg doping concentration ( $>10^{19} \text{ cm}^{-3}$ ) to achieve technically useful hole concentrations in the  $10^{17} \text{ cm}^{-3}$  range. At such high doping levels, the incorporation of nitrogen-vacancy-related compensating defects becomes favorable due to

their lowered formation energy.<sup>21,22,34,35</sup> This makes the formation of the impurity band a challenge. One approach for reducing the incorporation of nitrogen-vacancy-related compensating defects during growth is by enhancing the nitrogen chemical potential,<sup>22</sup> as was demonstrated for Mg:AlGaN.<sup>9</sup> As summarized in Fig. 3, the results by Bagheri *et al.*<sup>9</sup> show that the impurity band conduction is favored at high Mg doping and low compensation (depicted schematically in Fig. 2). For a Mg doping concentration of  $\sim 5 \times 10^{19} \text{ cm}^{-3}$ , an order of magnitude reduction in resistivity was observed for Mg-doped Al<sub>0.6</sub>Ga<sub>0.4</sub>N grown on single-crystal AlN substrates as compared to heteroepitaxial growth on sapphire.

First, the possible conduction mechanisms discussed above were studied in p-GaN; Fig. 4 shows the obtained resistivity and Hall data. To understand the impurity band transport in the relatively heavily doped GaN ( $5 \times 10^{19} \text{ cm}^{-3}$ ), it is useful to contrast it to a reference p-GaN sample doped with  $2 \times 10^{19} \text{ cm}^{-3}$  Mg, which showed the expected valence band transport behavior. Temperature dependence of the resistivity and Hall coefficient,  $R_H$ , of the reference sample both yielded the expected large ionization energy of  $\sim 150$  meV, Figs. 4(a) and 4(b). The estimated free hole concentration for the reference sample, assuming a pure valence band transport using the relation  $p = 1/qR_H$ , shows the expected thermal freeze out behavior corresponding to the relatively large Mg ionization energy, Fig. 4(c). A drastic difference was observed for the GaN sample doped with  $5 \times 10^{19} \text{ cm}^{-3}$  of Mg. The resistivity was found to be practically temperature-independent in the range of 150–400 K, and a shallow Mg ionization energy of 40 meV was observed above 400 K, Fig. 4(a). The measured Hall coefficient exhibited the expected trend for valence band transport at temperatures above 400 K but an opposite trend at lower temperatures, i.e., an increase in the free hole concentration with decreasing temperature; obviously, an anomalous result, Fig. 4(b).

The significantly reduced thermal dependence of resistivity and the anomalous trend reversal of  $R_H$  point to a transition from a valence-band- to an impurity-band-dominant conduction around 400 K. The Hall effect associated with impurity band conduction differs qualitatively and quantitatively from the quasi-free motion of holes in the valence band.<sup>36–38</sup> For valence band transport, the Hall scattering factor (the ratio of Hall and drift mobilities),  $A_{VB}$ , is  $\sim 1$ . For impurity band conduction, the Hall and drift mobilities can have different activation energies,<sup>31,38</sup> and therefore, the scattering factor,

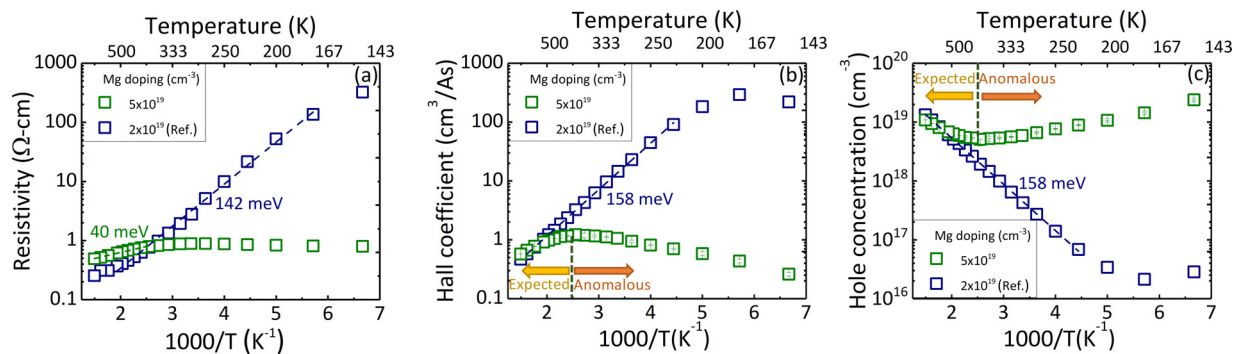


**FIG. 4.** Temperature-dependent (a) resistivity, (b) Hall coefficient, and (c) hole concentration for the p-GaN samples. The arrows in (b) and (c) show the expected and anomalous trends for the Hall coefficient and hole concentration for the  $5 \times 10^{19} \text{ cm}^{-3}$  doped sample. Note. The hole concentration in (c) is not the true free hole concentration and has been estimated for an assumption of pure valence band transport using the relation  $p = 1/qR_H$ .

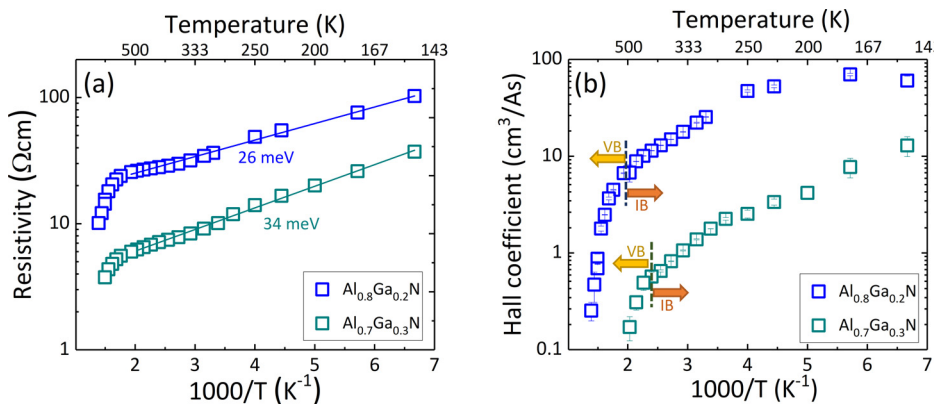


**FIG. 5.** Temperature-dependent (a) resistivity and (b) Hall coefficient for the Mg-doped Al-rich AlGaN samples. The arrows in (b) show the expected trend for valence band conduction (VB) and deviating trend from valence band conduction referred to as impurity band conduction (IB).

$A_{IB}$  is not equal to 1 and varies with temperature.<sup>38</sup> It has been shown that the sign and magnitude of  $A_{IB}$  depend on the geometric arrangement of sites involved in the carrier transfer process.<sup>36,38</sup> A negative  $A_{IB}$  was reported for p-GaN<sup>39</sup> and graded p-AlGaN.<sup>40</sup>

Generally, for a two-band transport, the Hall coefficient,  $R_H$ , depends on the respective resistivities of the two conduction mechanisms. In our case, the observed resistivity,  $\rho$ , consists of the valence band and impurity band resistivities, resulting in

$$\frac{1}{\rho} = \frac{1}{\rho_{VB}} + \frac{1}{\rho_{IB}}. \quad (1)$$

As such,

$$R_H = R_H^{VB} \left( \frac{\sigma_{VB}}{\sigma} \right)^2 + R_H^{IB} \left( \frac{\sigma_{IB}}{\sigma} \right)^2, \quad (2)$$

where  $R_H^{VB}$  and  $R_H^{IB}$  are the Hall coefficients for the valence and impurity band conduction, respectively, and are given by

$$R_H^{VB} = \frac{A_{VB}}{q P_{VB}}, \quad (3)$$

$$R_H^{IB} = \frac{A_{IB}}{q P_{IB}}. \quad (4)$$

At higher temperatures ( $>500$  K), where the valence band conduction dominates, the  $R_H$  behavior is qualitatively similar to the reference GaN sample. At lower temperatures, the net contribution of the valence band transport to  $R_H$  reduces exponentially due to the thermal freeze out of the free holes. This transition is captured in Eq. (2) and explains the anomalous trend in  $R_H$  at lower temperatures.

Figure 5 shows the temperature-dependent resistivity and Hall coefficient data obtained for Mg-doped AlGaN films with 70% and 80% Al content. The room temperature resistivities measured 9.7 and 37  $\Omega$  cm for  $Al_{0.7}Ga_{0.3}N$  and  $Al_{0.8}Ga_{0.2}N$ , respectively. These are the lowest resistivity values reported for high Al-content p-AlGaN and the first demonstration of technologically relevant p-type resistivity in 80% AlGaN.<sup>10,11</sup>

The resistivity data for both samples exhibited shallow activation energy of  $\sim 30$  meV below 500 K, much lower than the expected Mg ionization energy of  $>400$  meV, confirming the dominance of the impurity band conduction. The observed increase in the ionization

energy above 500 K suggests that the valence band transport becomes dominant at these temperatures. Figure 5(b) shows the temperature dependence of the Hall coefficient for these two samples: above 500 K, the  $R_H$  varies exponentially with temperature, a signature of valence band transport, while below 500 K, where the impurity band conduction dominates, the variation of  $R_H$  with temperature becomes more gradual. This is again attributed to the reduced contribution of  $R_H^{VB}$  to the net  $R_H$  value, as per Eq. (2). It is worth noting that if the impurity band conduction is neglected and the hole concentration is estimated using the relation  $p = A/qR_H$ , the ionization energy can appear to be systematically lower than the true ionization energy of the acceptor. The underestimation of  $R_H^{VB}$  would also lead to an erroneously high free hole concentration. This suggests that the contextual analysis of resistivity and Hall effect data is not straightforward in p-type ultrawide bandgap semiconductors, where the acceptors are deep and valence band conduction is limited. We suggest that a correct interpretation of the experimental data is only possible by extending the measurements to a wider temperature range.

In summary, by introducing a two-band conduction model, we were able to explain anomalous behavior of conductivity in high Al-content Mg:AlGaN grown on single-crystal AlN substrates. It was shown that while the impurity band conduction enables achieving lower resistivity than pure valence band conduction, it requires additional considerations in the interpretation of the Hall effect data. This arises from the fact that the Hall scattering factors for the impurity and valence band conduction are fundamentally different. While this study exemplifies the utility of impurity band conduction in overcoming the limitations in conventional p-type doping, it also points out that managing compensation is as important as in conventional doping. Record-low resistivities of 9.7 and 37  $\Omega$  cm were achieved in doping of bulk  $Al_{0.7}Ga_{0.3}N$  and  $Al_{0.8}Ga_{0.2}N$  films, respectively.

The authors gratefully acknowledge funding in part from AFOSR (Nos. FA9550-17-1-0225, FA9550-19-1-0114, and FA9550-19-1-0358), NSF (Nos. ECCS-1610992, ECCS-1508854, ECCS-1916800, and ECCS-1653383), and ARO (No. W911NF-16-C-0101).

## AUTHOR DECLARATIONS

### Conflict of Interest

The authors have no conflicts to disclose.

## Author Contributions

**Shashwat Rathkanthiwar:** Conceptualization (lead); Data curation (equal); Formal analysis (lead); Investigation (equal); Methodology (equal); Visualization (lead); Writing – original draft (lead); Writing – review & editing (equal). **Ramon Collazo:** Funding acquisition (equal); Project administration (equal); Resources (equal); Supervision (equal); Writing – review & editing (equal). **Zlatko Sitar:** Funding acquisition (equal); Project administration (equal); Resources (equal); Supervision (equal); Writing – review & editing (lead). **Pegah Bagheri:** Data curation (equal); Formal analysis (equal); Investigation (equal); Methodology (equal); Software (lead). **Dolar Khachariya:** Investigation (equal). **Seiji Mita:** Conceptualization (equal); Formal analysis (equal); Investigation (lead); Methodology (lead); Visualization (equal). **Cristyan Quinones-Garcia:** Investigation (supporting). **Yan Guan:** Investigation (supporting). **Baxter Moody:** Investigation (supporting); Validation (supporting). **Pramod Reddy:** Formal analysis (supporting); Validation (equal). **Ronny Kirste:** Funding acquisition (equal); Project administration (equal); Validation (equal).

## DATA AVAILABILITY

The data that support the findings of this study are available from the corresponding author upon reasonable request.

## REFERENCES

- <sup>1</sup>H. Amano, R. Collazo, C. D. Santi, S. Einfeldt, M. Funato, J. Glaab, S. Hagedorn, A. Hirano, H. Hirayama, R. Ishii, Y. Kashima, Y. Kawakami, R. Kirste, M. Kneissl, R. Martin, F. Mehneke, M. Meneghini, A. Ougazzaden, P. J. Parbrook, S. Rajan, P. Reddy, F. Römer, J. Ruschel, B. Sarkar, F. Scholz, L. J. Schowalter, P. Shields, Z. Sitar, L. Sulmoni, T. Wang, T. Wernicke, M. Weyers, B. Witzigmann, Y.-R. Wu, T. Wunderer, and Y. Zhang, *J. Phys. D* **53**, 503001 (2020).
- <sup>2</sup>R. Kirste, B. Sarkar, P. Reddy, Q. Guo, R. Collazo, and Z. Sitar, *J. Mater. Res.* **36**, 4638 (2021).
- <sup>3</sup>B. Sarkar, S. Mita, P. Reddy, A. Klump, F. Kaess, J. Tweedie, I. Bryan, Z. Bryan, R. Kirste, E. Kohn, R. Collazo, and Z. Sitar, *Appl. Phys. Lett.* **111**, 032109 (2017).
- <sup>4</sup>A. Klump, M. Hoffmann, F. Kaess, J. Tweedie, P. Reddy, R. Kirste, Z. Sitar, and R. Collazo, *J. Appl. Phys.* **127**, 045702 (2020).
- <sup>5</sup>S.-R. Jeon, Z. Ren, G. Cui, J. Su, M. Gherasimova, J. Han, H.-K. Cho, and L. Zhou, *Appl. Phys. Lett.* **86**, 082107 (2005).
- <sup>6</sup>H. Yu, E. Ulker, and E. Ozbay, *J. Cryst. Growth* **289**, 419 (2006).
- <sup>7</sup>A. Kalra, S. Rathkanthiwar, R. Muralidharan, S. Raghavan, and D. N. Nath, *Semicond. Sci. Technol.* **35**, 035001 (2020).
- <sup>8</sup>D. Nilsson, “Doping of high-Al-content AlGaN grown by MOCVD,” Ph.D. thesis (Linköping University Electronic Press, 2014).
- <sup>9</sup>P. Bagheri, A. Klump, S. Washiyama, M. Hayden Breckenridge, J. H. Kim, Y. Guan, D. Khachariya, C. Quiñones-García, B. Sarkar, S. Rathkanthiwar, P. Reddy, S. Mita, R. Kirste, R. Collazo, and Z. Sitar, *Appl. Phys. Lett.* **120**, 082102 (2022).
- <sup>10</sup>A. Jadhav, P. Bagheri, A. Klump, D. Khachariya, S. Mita, P. Reddy, S. Rathkanthiwar, R. Kirste, R. Collazo, Z. Sitar, and B. Sarkar, *Semicond. Sci. Technol.* **37**, 015003 (2022).
- <sup>11</sup>T. Kinoshita, T. Obata, H. Yanagi, and S. Inoue, *Appl. Phys. Lett.* **102**, 012105 (2013).
- <sup>12</sup>Y. Taniyasu, M. Kasu, and T. Makimoto, *Nature* **441**, 325 (2006).
- <sup>13</sup>A. Allerman, M. Crawford, M. Miller, and S. Lee, *J. Cryst. Growth* **312**, 756 (2010).
- <sup>14</sup>K. Ebata, J. Nishinaka, Y. Taniyasu, and K. Kumakura, *Jpn. J. Appl. Phys., Part 1* **57**, 04FH09 (2018).
- <sup>15</sup>W. Luo, B. Liu, Z. Li, L. Li, Q. Yang, L. Pan, C. Li, D. Zhang, X. Dong, and D. Peng, *Appl. Phys. Lett.* **113**, 072107 (2018).
- <sup>16</sup>X. Qiu, Y. Chen, E. Han, Z. Lv, Z. Song, and H. Jiang, *Mater. Adv.* **1**, 77 (2020).
- <sup>17</sup>X. Qiu, Y. Chen, E. Han, Z. Lv, Z. Song, and H. Jiang, *Mater. Adv.* **1**, 77 (2020).
- <sup>18</sup>A. Kausar, A. Osinsky, A. Dabiran, and P. Chow, *Appl. Phys. Lett.* **85**, 5275 (2004).
- <sup>19</sup>J. Simon, V. Protasenko, C. Lian, H. Xing, and D. Jena, *Science* **327**, 60 (2010).
- <sup>20</sup>R. Dalmau, B. Moody, R. Schlesser, S. Mita, J. Xie, M. Feneberg, B. Neuschl, K. Thonke, R. Collazo, A. Rice, J. Tweedie, and Z. Sitar, *ECS Trans.* **33**, 43 (2010).
- <sup>21</sup>A. Kalra, S. Rathkanthiwar, R. Muralidharan, S. Raghavan, and D. N. Nath, *IEEE Photonics Technol. Lett.* **31**, 1237 (2019).
- <sup>22</sup>C. Stampfl, J. Neugebauer, and C. G. Van de Walle, *Mater. Sci. Eng., B* **59**, 253 (1999).
- <sup>23</sup>Q. Yan, A. Janotti, M. Scheffler, and C. G. Van de Walle, *Appl. Phys. Lett.* **100**, 142110 (2012).
- <sup>24</sup>P. Reddy, S. Washiyama, F. Kaess, R. Kirste, S. Mita, R. Collazo, and Z. Sitar, *J. Appl. Phys.* **122**, 245702 (2017).
- <sup>25</sup>S. Washiyama, P. Reddy, B. Sarkar, M. H. Breckenridge, Q. Guo, P. Bagheri, A. Klump, R. Kirste, J. Tweedie, S. Mita, Z. Sitar, and R. Collazo, *J. Appl. Phys.* **127**, 105702 (2020).
- <sup>26</sup>M. L. Nakarmi, N. Nepal, J. Y. Lin, and H. X. Jiang, *Appl. Phys. Lett.* **94**, 091903 (2009).
- <sup>27</sup>P. Lu, R. Collazo, R. F. Dalmau, G. Durkaya, N. Dietz, B. Raghothamachar, M. Dudley, and Z. Sitar, *J. Cryst. Growth* **312**, 58 (2009).
- <sup>28</sup>D. Zhuang, Z. Herro, R. Schlesser, and Z. Sitar, *J. Cryst. Growth* **287**, 372 (2006).
- <sup>29</sup>A. Rice, R. Collazo, J. Tweedie, R. Dalmau, S. Mita, J. Xie, and Z. Sitar, *J. Appl. Phys.* **108**, 043510 (2010).
- <sup>30</sup>J. Tweedie, R. Collazo, A. Rice, J. Xie, S. Mita, R. Dalmau, and Z. Sitar, *J. Appl. Phys.* **108**, 043526 (2010).
- <sup>31</sup>E. F. Schubert, *Doping in III-V Semiconductors* (E. Fred Schubert, 2015).
- <sup>32</sup>L. Friedman and T. Holstein, *Ann. Phys.* **21**, 494 (1963).
- <sup>33</sup>H. Neumann, *Cryst. Res. Technol.* **23**, 1377 (1988).
- <sup>34</sup>B. Gunning, J. Lowder, M. Moseley, and W. A. Doolittle, *Appl. Phys. Lett.* **101**, 082106 (2012).
- <sup>35</sup>P. Reddy, Z. Bryan, I. Bryan, J. H. Kim, S. Washiyama, R. Kirste, S. Mita, J. Tweedie, D. L. Irving, Z. Sitar, and R. Collazo, *Appl. Phys. Lett.* **116**, 032102 (2020).
- <sup>36</sup>T. Holstein, *Philos. Mag.* **27**, 225 (1973).
- <sup>37</sup>D. Emin, *Philos. Mag.* **35**, 1189 (1977).
- <sup>38</sup>C. Chien and C. Westgate, *The Hall Effect and Its Applications* (Springer Science & Business Media, 2013).
- <sup>39</sup>Y. Kajikawa, *Phys. Status Solidi C* **14**, 1600129 (2017).
- <sup>40</sup>S. Rathkanthiwar, P. Bagheri, D. Khachariya, J. H. Kim, Y. Kajikawa, P. Reddy, S. Mita, R. Kirste, B. Moody, and R. Collazo, *Appl. Phys. Lett.* **121**, 072106 (2022).